# High-Density Fixed Point for Radially Compressed Single-Component Plasmas

J. R. Danielson, C. M. Surko, and T. M. O'Neil

*Department of Physics, University of California at San Diego, La Jolla, California 92093, USA*

(Received 27 April 2007; published 28 September 2007)

Rotating electric fields are used to compress electron plasmas confined in a Penning-Malmberg trap. Bifurcation and hysteresis are observed between low-density and high-density steady states as a function of the applied electric field amplitude and frequency. These observations are explained in terms of torque-balanced fixed points using a simple model of the torques on the plasma. Perturbation experiments near the high-density fixed point are used to determine the magnitude, frequency, and voltage dependence of the drive torque. The broader implications of these results are discussed.

DOI: 10.1103/PhysRevLett.99.135005 PACS numbers: 52.27.Jt, 52.25.Fi, 52.25.Kn, 52.55.Dy

Single-component plasmas in Penning-Malmberg traps have found many applications in science and technology, including atomic clocks, the trapping of antimatter, and the study of fundamental plasma processes [1–3]. Plasmas are confined by a uniform magnetic field and an axial electrostatic potential well. Plasma lifetimes are typically limited by small static asymmetries that produce a drag torque on the rotating plasma, causing its expansion. A particularly powerful tool to tailor these plasmas is the so-called "rotating wall" (RW) technique in which rotating electric field asymmetries are used to exert a torque in the direction of plasma rotation to increase confinement or produce radial compression of the plasma [4–6].

This technique is now used extensively for a variety of applications [3,7]. A recently discovered "strong-drive" regime provides new capabilities, including the ability to produce high-density steady states with plasma rotation frequencies very close to the RW frequency. The protocol for these experiments is such that the two control parameters of the system, RW frequency and RW amplitude, are set to fixed values; then the system is allowed to evolve freely to a new steady state. This is in contrast to most experiments (except Ref. [6]) where either the RW was tuned to a plasma mode or the amplitude changed slowly as the system evolves. These strong-drive experiments raise a number of questions, including the nature of the hysteresis and bifurcation observed between low- and high-density steady states [8,9].

In this Letter, models of the drive and drag torques are used to describe the stable, attracting fixed points of the system. Key ingredients are a drag torque due to a plasma mode resonance driven by static trap asymmetries and a RW drive torque that passes rapidly through zero as the plasma rotation frequency approaches the RW frequency. A number of tests of the model are described, including perturbation experiments to confirm the nature of the RW torque and to measure its magnitude near the high-density fixed point. Open questions for future research are discussed.

The apparatus and procedures for these experiments have been described previously [9]. Experiments are performed on electron plasmas in a cylindrical Penning-Malmberg trap aligned to the axis of a magnetic field, $B = 4.8$ T. Axial confinement is achieved by the application of $V_C = -100$ V on the end electrodes. One of the cylindrical electrodes is segmented azimuthally in order to apply the rotating electric fields. Radial density profiles are obtained by dumping trapped electron plasmas onto a phosphor screen and imaging with a camera. The perpendicular to parallel equilibration and rate of thermal conduction are rapid ($\tau < 1$ msec), so the plasma is well described by a single temperature, $T$, that is measured by a standard evaporation technique.

In equilibrium, the plasma density, $n$, is approximately constant; $n = N/\pi R_p^2 L_p$, with $N$ the total particle number, $R_p$ the plasma radius, and $L_p$ the plasma length. The radial plasma electric field causes it to rotate as a rigid rotor at the $E \times B$ drift frequency, $f_E = \mathrm{nec/B}$ [2]. The electrons bounce between the end potentials at a frequency, $f_b = v_{\mathrm{th}}/2L_p$, where $v_{\mathrm{th}} = (T/m)^{1/2}$ is the thermal velocity. For the plasmas discussed here, $f_E \gg f_b$, and $\nu_{ee} > f_b$, where $\nu_{ee}$ is the Coulomb collision frequency. Plasmas are compressed radially by the application of RW electric fields with frequency $f_{\mathrm{RW}}$, amplitude $V_{\mathrm{RW}}$, and azimuthal mode number $m_\theta = 1$, rotating in the same direction as the plasma [9].

Plasmas are trapped and allowed to equilibrate for $\sim$0.1 s. Then the RW fields, at fixed values of $f_{\mathrm{RW}}$ and $V_{\mathrm{RW}}$, are applied for a time $\Delta t$; and the plasma is dumped and imaged. Shown in Fig. 1 are the central density and the temperature as a function of time for $f_{\mathrm{RW}} = 7$ MHz and an applied RW, peak-to-peak voltage, $V_{\mathrm{RW}} = 1.2$ V. Also shown are radial profiles of the initial and final steady-state plasmas. The plasma temperature, initially $\sim$0.05 eV, rises to $\sim$2.8 eV during compression, then cools to $\sim$0.1 eV. For these conditions, the RW couples directly to the plasma and not to specific plasma modes.

For experiments over a broad range of $f_{\mathrm{RW}}$, and for $V_{\mathrm{RW}}$ sufficiently large, the RW torque can be used to compress the plasma until $f_E$ is very close to $f_{\mathrm{RW}}$ [8,9]. Experiments were also conducted in which the plasma was first compressed to some high density, then $f_{\mathrm{RW}}$ and/or $V_{\mathrm{RW}}$ were

 

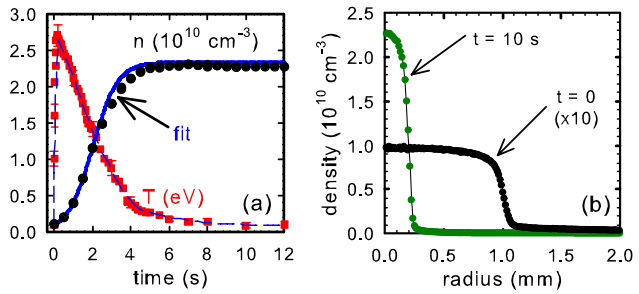


FIG. 1 (color online). (a) Density, $n$, and temperature, $T$, vs time during RW compression for $L_p = 11$ cm, $N = 3 \times 10^8$ electrons. Solid line is a fit described in the text. (b) Radial profiles before and after RW compression.

reduced. These compression and expansion experiments identified multiple stable fixed points and revealed two distinct types of hysteresis, one associated with changes in $f_{\mathrm{RW}}$ and another with changes in $V_{\mathrm{RW}}$. We show that both hysteresis effects are due to the same underlying phenomenon, namely, resonant coupling to a static asymmetry.

In Fig. 2(a), the final steady-state density is shown for a large value of $V_{\mathrm{RW}}$ over a broad range of $f_{\mathrm{RW}}$ (i.e., where both are held constant during the compression or expansion). When the plasma is compressed from low density, there is an impediment to reaching higher densities. The onset of this behavior [i.e., at $f_{\mathrm{RW}} \sim 1.0$ MHz in Fig. 2(a)] corresponds to the density at which a static field error drives a low-order Trivelpiece-Gould (TG) mode that propagates backwards on the rotating plasma column [9]. This mode, which is referred to as a zero-frequency mode (ZFM) since it is zero frequency (i.e., static) in the lab frame, produces an enhanced drag torque [10].

The TG dispersion relation shows that the frequency scales as $L_p^{3/2}$. Measurements for three different plasma

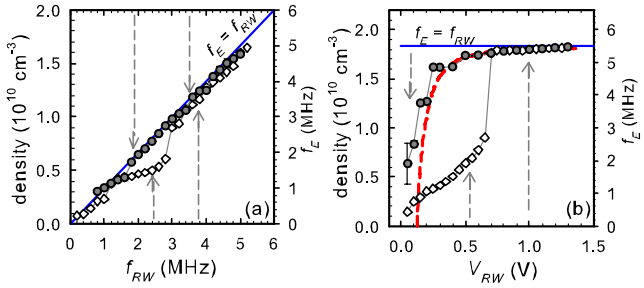


FIG. 2 (color online). (a) Final, steady-state densities for fixed values of $f_{\mathrm{RW}}$ at $V_{\mathrm{RW}} = 1.2$ V: (◇) compression from a low-density state; (●) expansion from a high-density state following compression at $f_{\mathrm{RW}} = 8$ MHz. (b) Steady-state density for fixed values of $V_{\mathrm{RW}}$ at $f_{\mathrm{RW}} = 5.5$ MHz: (◇) compression from a low-density state; (●) expansion following compression with $V_{\mathrm{RW}} = 1.3$ V applied for 20 s. A fit (red dotted line) to Eq. (2) is shown. Grey arrows indicate the path of the system in response to changes in (a) $f_{\mathrm{RW}}$ and (b) $V_{\mathrm{RW}}$; (blue solid line) indicate $f_E = f_{\mathrm{RW}}$. Here, $L_p = 20$ cm and $N = 3 \times 10^8$ electrons.

lengths verified this scaling [9] and identified the ZFM as the lowest-order TG mode possible, namely $m_\theta = 1, m_r = 1, m_z = 1$ (i.e., $k_z \sim \pi/L_p$). In contrast to the behavior in compression, as shown in Fig. 2(a), when the plasma is expanded from a high-density state, the plasma reaches $f_E \approx f_{\mathrm{RW}}$ over the entire range of $f_{\mathrm{RW}}$.

As illustrated in Fig. 2(b), for frequencies outside this region of hysteresis, a second hysteresis phenomenon is observed as $V_{\mathrm{RW}}$ is varied. A bifurcation to a high-density steady state is observed when the value of $V_{\mathrm{RW}}$ used to compress the plasma is increased. Once in the high-density state, the plasma can be maintained in this state at significantly smaller drive amplitudes. As described below, this behavior is also due to the ZFM resonance. Similar hysteretic behavior associated with ZFM resonances was observed previously in laser-cooled ion clouds [11]. However, in those experiments, the control parameter (laser frequency, equivalent to $V_{\mathrm{RW}}$ here) was varied continuously in order to change the plasma rotation frequency.

To understand these effects, we develop a model to describe the attracting fixed points of the system. The plasma is assumed to be a rigid rotor, described by two parameters: the plasma rotation frequency $f_E$ (i.e., $f_E \propto n$) and the temperature $T$ [2]. When the plasma is cold, the total plasma angular momentum is given by $P_\theta \approx -(eNB/4c)R_p^2 \approx -(e^2N^2/4\pi L_p)/f_E$ [2]. In this approximation (relevant to the high-density fixed point), the torque $\mathcal{T} = dP_\theta/dt$ is a function of $f_E$.

We focus on the three dominant torques acting on the plasma. In addition to the applied RW torque, $\mathcal{T}_{\mathrm{RW}}$, two drag torques act to slow the plasma rotation and increase the plasma radius. There is a background drag torque, $\mathcal{T}_B$, causing the plasma to expand at all densities [5,9]. In addition, the sharp ZFM produces a large torque, $\mathcal{T}_Z$, near the density at which this mode is resonant. The total torque on the plasma, $\mathcal{T}$, can be written as

$$\mathcal{T} = \eta \frac{f_{\mathrm{RW}} - f_E}{f_E} V_{\mathrm{RW}}^2 - \frac{\beta f_E}{D^2 + f_E^2} - \frac{\gamma(\delta f_0)}{(f_E - f_0)^2 + (\delta f_0)^2}, \tag{1}$$

where the three terms are respectively $\mathcal{T}_{\mathrm{RW}}$, $\mathcal{T}_B$, and $\mathcal{T}_Z$, with constants $\eta$, $\beta$, $\gamma > 0$; the parameter $D$ is discussed below. The torques $\mathcal{T}_B$ and $\mathcal{T}_Z$ are written with explicit negative signs, since they are drag torques at all densities. Elements of Eq. (1) are similar to those used in Ref. [12] to describe the hysteresis observed in laser compression of ion plasmas [11]. An important difference is that, in the RW case discussed here, the drive torque is proportional to $f_{\mathrm{RW}} - f_E$. As shown below, this model explains in a natural way the hysteresis as a function of both control parameters, $f_{\mathrm{RW}}$ and $V_{\mathrm{RW}}$.

Equation (1) is motivated by the following considerations. For $\Delta f = f_{\mathrm{RW}} - f_E \ll f_{\mathrm{RW}}$ (relevant to the high-density steady state), a perturbation analysis predicts that the drive torque, $\mathcal{T}_{\mathrm{RW}}$, is linear in $\Delta f$ and quadratic in $V_{\mathrm{RW}}$

[13]. This torque compresses the plasma when $f_{\mathrm{RW}} > f_E$, and causes expansion when $f_{\mathrm{RW}} < f_E$ [2]. Further, assuming the RW field acts only in a Debye sheath at the plasma edge, $\mathcal{T}_{\mathrm{RW}} \propto R_p^2 \propto 1/n \propto 1/f_E$. This assumes $L_p \sim$ constant during compression, which is a good approximation when $R_p \ll R_w \ll L_p$. The coupling constant, $\eta$, in Eq. (1) is independent of $n$, but may depend on $T$ and $L_p$. Although this form of $\mathcal{T}_{\mathrm{RW}}$ is strictly valid only for $\Delta f \ll f_{\mathrm{RW}}$, as discussed below, it is approximately correct over the parameter range of interest. While $\mathcal{T}_{\mathrm{RW}}$ could be modified to include resonant coupling of the RW to TG modes [5,14], they do not appear to be important in the "strong-drive" regime.

The background drag torque, $\mathcal{T}_B$, was measured by examining the rate of plasma expansion with $V_{\mathrm{RW}} = 0$. The expansion rate, $\Gamma_o(n) = (1/n)dn/dt$, changes with $n$, from $\Gamma_o \propto n^2$ at low densities to $\Gamma_o \propto n^0$ for $n \gtrsim 5 \times 10^9$ cm$^{-3}$ [9]. Since $\mathcal{T}_B = dP_\theta/dt \propto 1/n^2(dn/dt) \propto (1/n)\Gamma_o(n)$, $\mathcal{T}_B$ increases with $n$ at lower densities, reaches a maximum, and then decreases as $1/n$ at higher densities. This motivates the empirical parametrization of $\mathcal{T}_B$ in the second term in Eq. (1), where experiments show the crossover point $D \propto (T/L_p)^{1/2}$ [9]. The drag torque, $\mathcal{T}_Z$, due to the ZFM, is modeled by a single Lorentzian centered at $f_0$ with width $\delta f_0 \ll f_0$.

Figure 3 illustrates the bifurcation and hysteresis behavior predicted by Eq. (1). Here $\mathcal{T}$ is separated into two components: the RW torque, $\mathcal{T}_{\mathrm{RW}}$, and the total drag torque, $\mathcal{T}_d = \mathcal{T}_B + \mathcal{T}_Z$, which includes a ZFM at $f_0 = 1.4$ in the arbitrary units of the figure. Figures 3(a) and 3(b) show torque curves versus $f_E$ (i.e., $f_E \propto n$) for a range of $f_{\mathrm{RW}}$ and $V_{\mathrm{RW}}$. The fixed points at $\mathcal{T} = 0$ (i.e., where $\tau_{\mathrm{RW}} = -\mathcal{T}_d$) are candidates for the observed steady states. The stability of the fixed points is determined by the sign of $d\mathcal{T}/dn$, namely, whether the torque causes the system to move toward ($d\mathcal{T}/dn < 0$) or away from ($d\mathcal{T}/dn > 0$) the fixed point [2].

Figures 3(c) and 3(d) show $f_E$ for these stable and unstable fixed points (solid and open circles) as a function of $f_{\mathrm{RW}}$ and $V_{\mathrm{RW}}$, respectively. As shown in Fig. 3(c), the value of $f_E$ for the stable states increases much less rapidly with increasing $f_{\mathrm{RW}}$ as the ZFM resonance is approached from below. In contrast, as $f_{\mathrm{RW}}$ is decreased from above, the ZFM has little effect on the transition to lower densities. As shown in Fig. 3(d), the value of $f_E$ for the lower stable fixed point increases only slowly as a function of $V_{\mathrm{RW}}$ near the ZFM until $V_{\mathrm{RW}} \gtrsim 0.4$. Above this value, the lower fixed point disappears, and the system is attracted to the high-density fixed point. In contrast, once in the high-density state, this state disappears only at a much lower amplitude ($V_{\mathrm{RW}} < 0.2$).

The experimental results in Figs. 2(a) and 2(b) correspond well to the behavior shown in Figs. 3(c) and 3(d). The hysteresis and bifurcation arise from the fact that, due to the ZFM resonance, there is more than one stable fixed point for a range of values of $f_{\mathrm{RW}}$ and $V_{\mathrm{RW}}$. The steep slope of the torque curve near $f_{\mathrm{RW}} = f_E$ and the smaller slope of the drag torque explain in a natural way the fact that $f_{\mathrm{RW}} \approx f_E$ near the high-density fixed point. Discrepancies between the model and experimental results are likely due to the neglect of temperature effects (e.g., heating is expected to broaden the ZFM resonance).

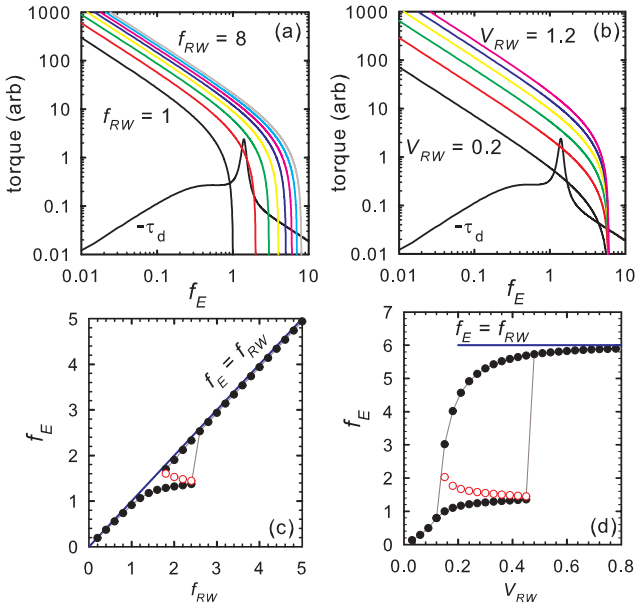


FIG. 3 (color online). Schematic illustration of the model (in arbitrary units): (a) $\mathcal{T}_{\mathrm{RW}}$ for different frequencies with $V_{\mathrm{RW}} = 1.0$ and a drag-torque curve, $-\mathcal{T}_d$, including a single ZFM at $f_0 = 1.4$, plotted as a function of $f_E$; (b) $\mathcal{T}_{\mathrm{RW}}$ for different amplitudes with $f_{\mathrm{RW}} = 6.0$; (c), (d) the corresponding stable (●) and unstable (○) fixed points (i.e., $\mathcal{T} = 0$) for a range of $f_{\mathrm{RW}}$ and $V_{\mathrm{RW}}$, respectively.

Beyond the form of the hysteresis in $V_{\mathrm{RW}}$ and $f_{\mathrm{RW}}$, several other predictions of Eq. (1) can be compared to the results of experiments. First, the steady-state density near the high-density fixed point can be described by setting $\mathcal{T} = 0$ and assuming $f_{\mathrm{RW}} - f_0 \gg \delta f_0$ (i.e., ZFM effects are negligible) and $f_E \gg D$ to find,

$$f_E \approx f_{\mathrm{RW}} - \frac{\beta}{\eta V_{\mathrm{RW}}^2}. \tag{2}$$

The prediction of Eq. (2) is shown by the dashed line in Fig. 2(b) and is in good agreement with the data. This fit and measurement of the drag torque, $\mathcal{T}_B \approx \beta/f_E \approx 1.1$ eV, taken with the RW drive off [8], provide a quantitative measure of $\eta$ and thus $\mathcal{T}_{\mathrm{RW}}$. From the data of Fig. 2(b) and Eq. (2), we find $\eta = 59 \pm 9$ eV/V$^2$. Using these values, the data in Fig. 2 at $V_{\mathrm{RW}} = 1.0$ V correspond to $f_{\mathrm{RW}} - f_E \approx 0.1$ MHz (i.e., $\Delta f/f \sim 0.02 \ll 1$), thus confirming that $\Delta f/f \ll 1$ near the high-density fixed point. We note that the precision of this fit exceeds greatly that possible by direct measurement of the plasma density.

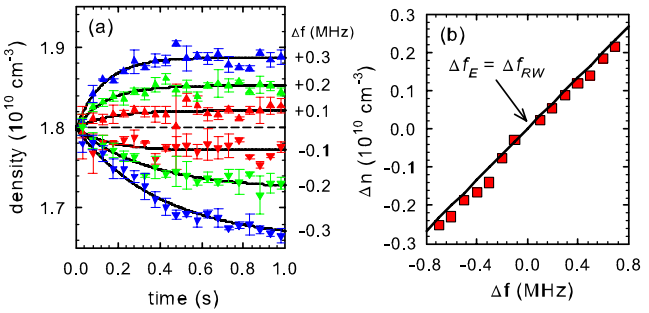


FIG. 4 (color online). (a) Density vs time following changes in $f_{\mathrm{RW}}$ from the initial value, $f_{\mathrm{RW}} = 5.5$ MHz, for $V_{\mathrm{RW}} = 1.0$ V. Solid lines are fits to the data, used to determine $R$ and $\Delta n$. (b) $\Delta n$ as a function of $\Delta f_{\mathrm{RW}}$.

The plasma response to perturbations near the high-density fixed point provides further tests of the model. From Eq. (2), if $f_{\mathrm{RW}}$ is changed by an amount $\Delta f_{\mathrm{RW}}$, then $\Delta f_E = \Delta f_{\mathrm{RW}}$. Recalling the relationship between $P_\theta$ and $f_E$, the plasma response can be written

$$\frac{df_E}{dt} \approx \frac{4\pi L_p f_E}{e^2 N^2}[\eta(f_{\mathrm{RW}} + \Delta f_{\mathrm{RW}} - f_E)V_{\mathrm{RW}}^2 - \beta]. \quad (3)$$

If the plasma is initially in a steady state, Eq. (3) indicates that the initial rate of change of the density will be proportional to $\Delta f_{\mathrm{RW}}$, providing a second measure of the drive torque, this one independent of $\mathcal{T}_B$.

In Fig. 4, plasmas were compressed to the high-density steady state by applying the RW for 20 s, then $f_{\mathrm{RW}}$ was changed by an amount $\Delta f_{\mathrm{RW}}$. From the fits to the resulting time evolution shown in Fig. 4(a), two parameters can be extracted: the magnitude, $\Delta n$, of the steady-state density change, shown in Fig. 4(b), and the response rate, $R$, where $df_E/dt|_{t=0} \equiv R\Delta f_{\mathrm{RW}}$. The agreement between the data and the prediction, $\Delta f_E = \Delta f_{\mathrm{RW}}$, further confirms the properties of the torque model. The noticeable asymmetry with $\pm\Delta f$ in Fig. 4(a) is not contained in the model. It may be due to the fact that the RW couples to the plasma edge, so plasma expansion and compression proceed differently.

The fits in Fig. 4(a) for $\Delta f_{\mathrm{RW}}/f_{\mathrm{RW}} < 0.1$ yield a response rate $R = 6.4 \pm 1$ s$^{-1}$. Equation (3), for $L_p = 20$ cm, $N = 3 \times 10^8$, $V_{\mathrm{RW}} = 1.0$ V and this value of $R$ provides a second value of the torque coefficient, $\eta = 63 \pm 10$ eV/V$^2$, which is in good agreement with $\eta = 59 \pm 9$ eV/V$^2$ from the fit in Fig. 2(b).

Near the high-density fixed point the RW drive and asymmetry torques provide relatively small perturbations. In contrast, plasma heating by the RW is a major effect during compression. Shown in Fig. 1(a) is a fit to $n(t)$ including the relevant temperature-dependent terms in $P_\theta$ [2]. The measured response rate during compression, $R \approx 1.5$ s$^{-1}$, is a factor of 4 less than that measured near the high-density fixed point. Given that the plasma evolves slowly on thermal-equilibration time scales, it will be of interest to determine whether the compression dynamics can be described within the framework of thermodynamics [2,12,13].

The results presented here provide an understanding of the high-density, strong-drive regime of RW compression and (qualitatively) the transition to and from it. Key ingredients are the inclusion in Eq. (1) of a sharp ZFM resonance, which causes the observed hysteresis and determines the low-density fixed point, and the form of $\tau_{\mathrm{RW}}$, which passes rapidly through zero at $f_{\mathrm{RW}} = f_E$ and determines the high-density fixed point. The ZFM resonance provides a barrier to reaching the high-density fixed point that can be overcome if the RW torque is sufficiently strong. We note that the model presented here is relatively insensitive to the details of the RW and background drag torques away from the high-density fixed point; any relatively smooth model for $\mathcal{T}_{\mathrm{RW}}$ or $\mathcal{T}_B$ would give qualitatively similar results.

This work was supported by NSF Grant No. PHY 03-54653. We wish to acknowledge discussions with M. W. Anderson on theoretical aspects of this work and E. A. Jerzewski for his expert technical assistance.

[1] J. J. Bollinger, D. J. Wineland, and D. H. E. Dubin, Phys. Plasmas **1**, 1403 (1994).
[2] D. H. E. Dubin and T. M. O'Neil, Rev. Mod. Phys. **71**, 87 (1999).
[3] C. M. Surko and R. Greaves, Phys. Plasmas **11**, 2333 (2004).
[4] X.-P. Huang, F. Anderegg, E. M. Hollmann, C. F. Driscoll, and T. M. O'Neil, Phys. Rev. Lett. **78**, 875 (1997).
[5] E. M. Hollmann, F. Anderegg, and C. F. Driscoll, Phys. Plasmas **7**, 2776 (2000).
[6] R. G. Greaves and C. M. Surko, Phys. Rev. Lett. **85**, 1883 (2000); Phys. Plasmas **8**, 1879 (2001).
[7] L. V. Jorgensen *et al.*, Phys. Rev. Lett. **95**, 025002 (2005).
[8] J. R. Danielson and C. M. Surko Phys. Rev. Lett. **94**, 035001 (2005).
[9] J. R. Danielson and C. M. Surko, Phys. Plasmas **13**, 055706 (2006).
[10] R. Keinigs, Phys. Fluids **27**, 1427 (1984).
[11] D. J. Heinzen, J. J. Bollinger, F. L. Moore, W. M. Itano, and D. J. Wineland, Phys. Rev. Lett. **66**, 2080 (1991).
[12] T. M. O'Neil and D. H. E. Dubin, Phys. Plasmas **5**, 2163 (1998).
[13] M. W. Anderson and T. M. O'Neil, Bull. Am. Phys. Soc. **51**, 248 (2006).
[14] Y. Soga, Y. Kiwamoto, and N. Hashizume, Phys. Plasmas **13**, 052105 (2006).